Asian Journal of Information Technology 6 (11): 1160-1166, 2007
ISSN: 1682-3915
© Medwell Journals, 2007

Mathematical Modeling of Wind Energy Systems

[1]V. Ramakrishnan and [2]S.K. Srivatsa
[1]Department of EEE, University of Vinayaka Missions, AVIT, Chennai, 603 104, India
[2]Department of ICE, St. Joseph's College of Engineering, Chennai, 600 119, India

Abstract: The development of wind energy systems and advances in power electronics, have enabled efficient future for wind energy. Our simulation study carried out at Chennai, India during last year compares three control schemes used in wind energy systems. Three methods widely used control schemes for wind energy systems are: Pitch control, Rotor Resistance control and Vector control of double fed induction generators. Their effectiveness in controlling the fluctuations in the output power occurring due to speed variations have been investigated. The mathematical model built in SIMULINK to simulate the systems is described. The control system design for the power control mathematical model is discussed and the report concludes with an analysis of the simulation results comparing the three control techniques.

Key words: Wind energy systems, control schemes, SIMULINK

INTRODUCTION

Rising pollutions levels and worrying changes in climates, arising in great part from energy production processes demand the reduction of ever-increasing environmentally damaging emission. In recent years, there has been an increase in the use of renewable energy sources due to growing concern for the pollution caused by fossil-fuel-based energy. Harnessing clean energy sources like the sunlight and wind to produce electricity decreases the dependency on fossil-fuel and enables electrical energy generation with minimal pollution.

These environmentally friendly technologies in particular require in suitable development period to establish themselves in a market place of high technical standards. The world wide potential of wind power means that its contribution to electricity productions can be of significant proportions. The themes developed in the present work are therefore, particularly concerned with this topic.

The mathematical modeling of the various components of a typical wind system and their implementation in SIMULINK traditional wind energy system consist of a stall-regulated or pitch control turbine connected to a synchronous generator through gear box. The synchronous generator at fixed speed and one of the earliest rotor control schemes was the rotor resistance control. The speed of the induction machine is controlled by the changing the external resistance in the rotor circuit. The drawback of the above two methods, does not enable wind power capture at low wind speeds.

The double fed induction machine is an extension of the slip-power recovery scheme, wherein the converter and the rectifier on the rotor side are replaced by bi-directional converters. By injecting currents into the rotor, the machine can be made to act like a generator at both sub-synchronous and super-synchronous speeds. Power factor control at the grid side can by obtained by controlling the grid side converter. Three methods can be used for constant desired output and they are described in the study.

Variations for different control output power reference are compared and the methods are evaluated based on the response time and the magnitude of change in the output power compared to the desired output power and also compared by simulation in SIMULINK. We conclude that the doubly fed induction generator is the best one when compared with other two methods.

TYPICAL WIND TURBINE GENERATOR

The basic components involved in the representation of a typical wind turbine generator are shown in Fig. 1.

The entire wind energy system can be sub divided into following components:

- Model of the wind
- Turbine model
- Shaft and gearbox model
- Generator model
- Control system model

Corresponding Author: V. Ramakrishnan, Department of EEE, University of Vinayaka Missions, AVIT, Chennai, 603 104, India

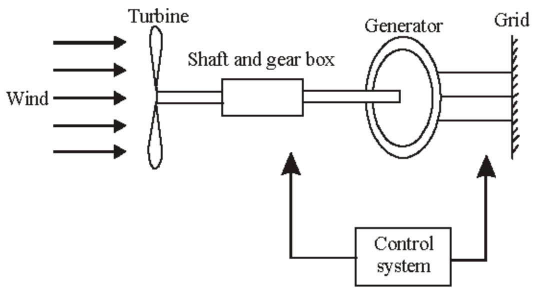

Fig. 1: Components of a typical wind system

The first three components form the mechanical part of the wind turbine generator. The generator forms the electro-mechanical link between the turbine and the power system and the control system controls the output of the generator. The control system model includes the actuator dynamics involved, be it the hydraulics controlling the pitch of the blades, or the converters controlling the induction generator.

This study describes the mathematical modeling of the various components of the wind system and their implementation in SIMULINK Manual (1997).

Model of the wind: The model of the wind should be able to simulate the temporal variations of the wind velocity, which consists of gusts and rapid wind speed changes.
The wind velocity (Vw) can be written as

$$V_w = V_{wB} + V_{wG} + V_{wR} \qquad (1)$$

Where,
V_w = Total wind velocity.
V_{wB} = Base wind velocity.
V_{wG} = Gust wind component.
V_{wR} = Ramp wind component.

The base wind speed is a constant and is given by

$$V_{wB} = C_1 \; C_1\text{: constant} \qquad (2)$$

The gust component is represented as a (1-cosine) term and is given by

$$V_{wg} = \begin{cases} 0 & t < T_1 \\ C_2\left\{1-\cos\left[\pi\frac{t-T_1}{T_2-T_1}\right]\right\} & T_1 \le t \le T_2 \\ 0 & t > T_2 \end{cases} \qquad (3)$$

Where, C_2 is the maximum value of the gust component and T_1 and T_2 are the start and stop times of the gust, respectively.

The rapid wind speed changes are represented by a ramp function and are given by

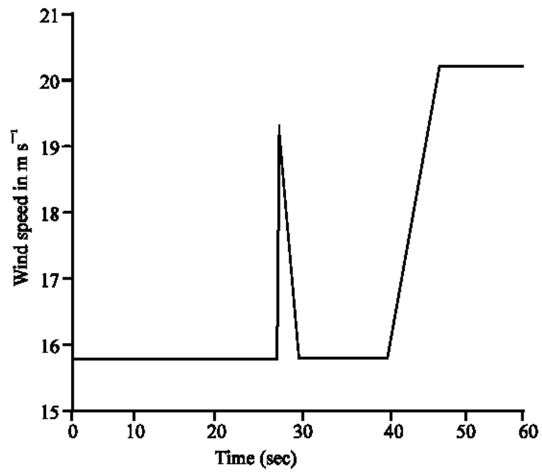

Fig. 2: Wind speed profile used for simulation

$$V_{wR} = \begin{cases} 0 & t < T_3 \\ C_3\left[\pi\frac{t-T_3}{T_4-T_3}\right] & T_3 \le t \le T_4 \\ 0 & t > T_4 \end{cases} \qquad (4)$$

Where C_3 is the maximum change in wind speed caused by the ramp and T_3 and T_4 are the start and stop times of the ramp, respectively.

The noise component of the wind speed is not modeled as the large turbine inertia does not respond to these high frequency wind speed variations.

The wind speed profile used to compare the three power control methods is shown in Fig. 2.

TURBINE MODEL

$$Ww = V_a\,\rho/2\,(v_1^2 - v_3^2)$$

Wind turbine power Pw =

$$\frac{dw_w}{dt} = \frac{dV_a\,\rho/2\,(v_1^2 - v_3^2)}{dt}$$

An air volume flow in the rotor area

$$(A_2 = A_R) \text{ of } \frac{dv_a}{dt} = A_R V_2$$

Yields in the quasi-steady state

$$Pw = A_R\,\rho/2\,(v_1^2 - v_3^2)\,V_2$$

According to BetZ, the maximum wind turbine power output (Siegfried *et al*., 2006).

P_m = $16/27\, A_R\, \rho/2\, V_1^3$ is obtained when
V_2 = $2/3\, V_1$ and $V_3 = 1/3\, V_1$

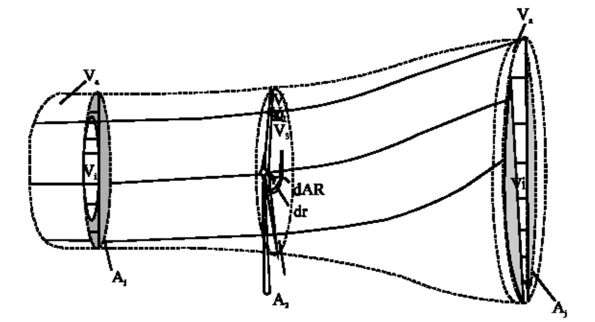

Fig. 3: Airstream around a turbine

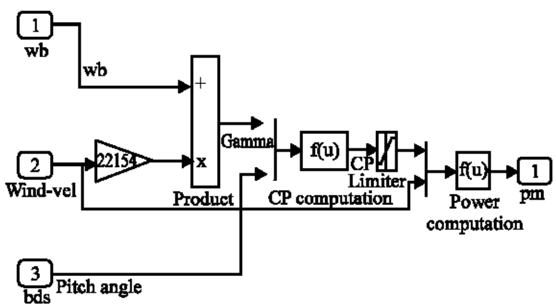

Fig. 4: SIMULINK implementation of the wind turbine model

The turbine model (Fig. 3) represents the power captured by the turbine. The ratio of the power Pw absorbed by the turbine to that of moving air mass (Pw) in an area A is given by

$$P_w = 1/2\ \rho\ Av^3_w;\ A_R = A \tag{5}$$

Where, ρ is the density of air.

However, the turbine captures only a fraction of this power. The power captured by the turbine (P_m) can be expressed as

$$P_m = P_w \times Cp \tag{6}$$

Where Cp is a fraction called the power coefficient. The power coefficient represents the fraction of the power in the wind captured by the turbine and has a theoretical maximum of 0.55.

The power coefficient can be expressed by a typical empirical formula as

$$Cp = 1/2\ (\gamma - 0.022\ \beta^2 - 5.6\ )\ e^{-0.17\gamma} \tag{7}$$

Where β is the pitch angle of the blade in degrees and γ is the tip speed ratio of the turbine, defined as.

$$\gamma = \frac{v_w\,(mph)}{\omega_b\,(rad\ s^{-1})}\ (\omega b\text{: turbine angular speed}) \tag{8}$$

Equation 5-8 describe the power captured by the turbine and constitute the turbine model.

The SIMULINK implementation of the turbine model is shown in Fig. 4.

SHAFT AND GEARBOX MODEL

The turbine is connected to the rotor of the generator through a gearbox. The gearbox is used to step up the low angular speeds of the turbine (normally about 25-30 rpm) to the high rotational speeds of the generator (normally around 1800 rpm). Figure 5 shows the shaft and gearbox model, with all the torques acting on the system and the angular velocities of the various masses (Tony *et al.*, 2001).

The turbine torque T_m (produced by the wind), accelerates the turbine inertia and is counterbalanced by the shaft torque T_{s1} (produced by the torsion action of the 0 speed shaft). Thus,

$$T_m - T_{s1} = J_m \frac{d\omega_b}{d_t} \tag{9}$$

Where ω_b = angular velocity of the turbine and J_m = inertia of the turbine.

Similarly, the shaft torque produced by the high speed shaft (T_{s2}) accelerates the rotor and is counterbalanced by the electromagnetic torque (T_e) produced by the generator.
Thus,

$$T_{s2} - T_e = J_r \frac{d\omega_r}{dt} \tag{10}$$

Where ω_r = angular velocity of the rotor and J_r = inertia of the rotor.

Assuming that the gearbox is ideal, with no backlash or losses and assuming that the shafts are rigid,

$$\frac{T_{s1}}{T_{s2}} = \frac{\omega_r}{\omega_b} = \frac{n_1}{n_2} \tag{11}$$

Where n_1/n_2 = gearbox ratio.

Eliminating the shaft torques from Eq. 9 and 10 using 11, we get

$$T_m\left[\frac{n_2}{n_1}\right] - T_e = \left[\underbrace{J_m\left[\frac{n_2}{n_1}\right]^2 + J_r}_{J_{eq}}\right]\frac{d\omega_r}{dt} \tag{12}$$

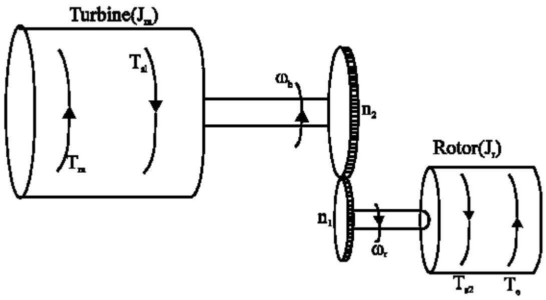

Fig. 5: Shaft and gearbox model

INDUCTION GENERATOR MODEL

The three control schemes-pitch control, rotor resistance control and vector controlled doubly fed induction machine-use different induction machines and different excitations for operation. The pitch control scheme uses a squirrel cage induction machine, in which the rotor circuit is short-circuited. The rotor resistance control method utilizes a wound rotor induction machine and the doubly fed induction generator uses a rotor-current-controlled wound rotor machine.

Since SIMULINK is an equation solver, different machine models must be used depending on the inputs to the system. However, only minor modifications are required in the standard induction machine model to obtain the three different models.

STANDARD INDUCTION MACHINE MODEL

The induction machine model is modeled in the synchronously rotating reference frame, rotating at the synchronous speed ω_s. The block diagram representation of the machine model is shown in Fig. 6.

Conversion from abc to dq quantities: For the stator, the stator quantities (stator voltage is used for further derivations) in the stationary reference frame fixed to the stator (α -β frame) can be expressed as a space vector given as Sergey (2005)

$$\overline{v}_s(\alpha\beta) = 2/3\ [v_{sa}(t)+av_{sb}(t)+a^2\ v_{sc}(t)] \qquad (13)$$

$$\overline{v}_s(\alpha\beta) = v_{\alpha s} + jv_{\beta s} \qquad (14)$$

Where, $v_s(\alpha\beta)$ = time-varying stator voltage space vector, $v_{sa}(t)$, $v_{sb}(t)$, $v_{sc}(t)$ = three phase voltage applied to the stator.

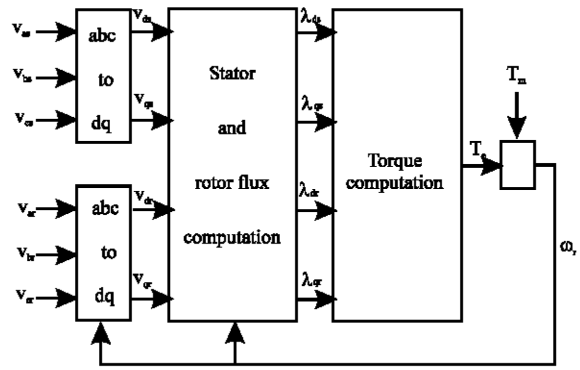

Fig. 6: Block diagram representation of the induction machine model

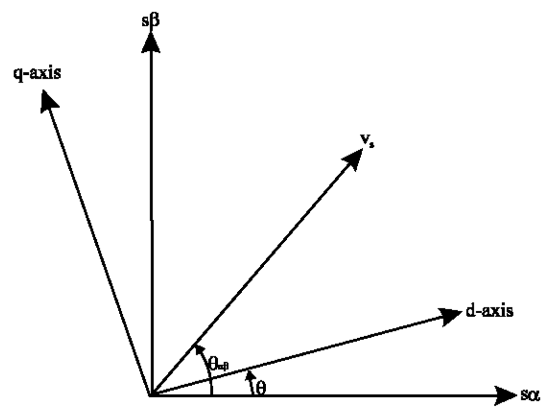

Fig. 7: Space vector diagram for stator quantities

$$a = e^{j\frac{2\pi}{3}};\ (j=\sqrt{-1})$$

And $v_{\alpha s}$, $v_{\beta s}$, = real and imaginary parts of $\overline{v}_{s(\alpha\beta)}$, respectively.

The space vector diagram showing the stator voltage and the reference frames is shown in Fig. 7.

The d-q axes shown, correspond to the synchronously rotating reference frame, which is the common frame of reference for the stator quantities. Since the d-q axes rotate at synchronous speed, the angleθ can be expressed as

$$\theta(t) = \theta_0 + \int_0^t \omega_s\, d\tau \qquad (15)$$

Where, θ_0 = initial angle of the d-q frame w.r.t the α-β frame.

Expressed in the d-q reference frame, the stator voltage space vector can be written as

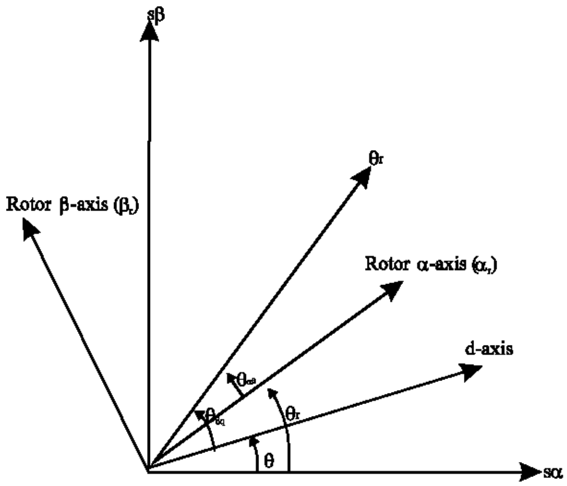

Fig. 8: Space vector diagram for the rotor quantities

$$\bar{v}_s(dq) = |\bar{v}_s(\alpha\beta)|e^{j}(\theta^{\alpha\beta-\theta}) \quad (16)$$

$$\Rightarrow \bar{v}_s(dq) = \bar{v}_s(\alpha\beta)e\text{-}^{\theta j} \quad (17)$$

Rewriting Eq. 17 in a matrix form, using

$$\bar{v}_s\, dq) = v_{ds} + j\, v_{qs} \quad (18)$$

the following transformation is obtained.

$$\begin{pmatrix} v_{ds} \\ v_{qs} \end{pmatrix} = \begin{pmatrix} \cos\theta & \sin\theta \\ -\sin\theta & \cos\theta \end{pmatrix} \begin{pmatrix} v_{\alpha s} \\ v_{\beta s} \end{pmatrix} \quad (19)$$

The rotor quantities (rotor voltage are used for further derivations) can similarly be expressed in the stationary frame fixed to the rotor as

$$\bar{V}_{r(\alpha r\beta r)} = 2/3[v_{ra}\,(t) + a\, v_{rb}\,(t) + a^2\, v_{rc}\,(t)] \quad (20)$$

Where, $\bar{v}_{r(\alpha r\beta r)}$ = time varying rotor flux vector in the rotor a - β frame and v_{ra} (t), v_{rb} (t), v_{rc} (t) = three phase voltage applied to the rotor.

Figure 8 shows the rotor voltage space vector along with the rotor reference frame, the d-q reference frame and the stator a-axis (used as the reference for measuring the angles).

Since the rotor rotates at an angular speed of ω_r w.r.t the stator,

$$\theta_r = \theta_{r0} + \int_0^t \omega_r\, d\tau \quad (21)$$

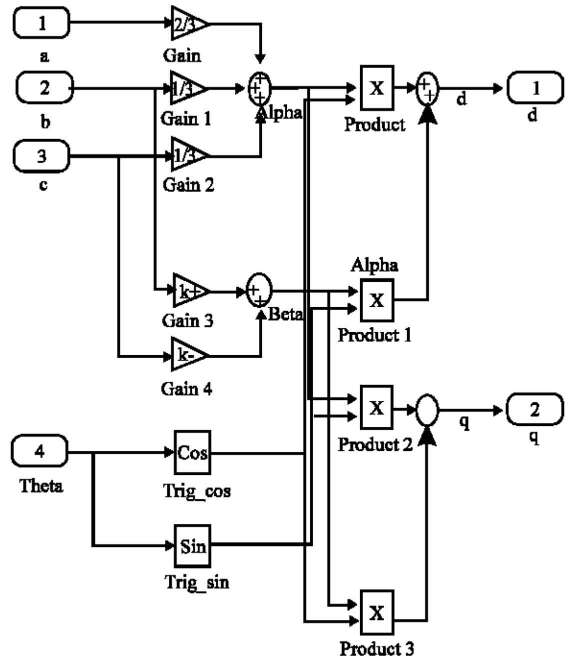

Fig. 9: ABC to DQ conversion

Where, θ_{r0} = initial angle of the rotor w.r.t the stator α axis.

The rotor voltage space vector can be expressed in the d-q reference frame as

$$\begin{aligned} \bar{v}_{r(dq)} &= \left|\bar{v}_{r(\alpha r \beta r)}\right| e^{j\theta dq} \\ &= \left|\bar{v}_{r(\alpha r \beta r)}\right| e^{j(\theta\alpha\beta + \theta r - \theta)} \end{aligned} \quad (22)$$

$$\bar{v}_{r(dq)} = \bar{v}_{r(\alpha r \beta r)} e^{-j(\theta - \theta r)} \quad (23)$$

Rewriting in matrix notation.

$$\begin{pmatrix} v_{dr} \\ v_{qr} \end{pmatrix} = \begin{pmatrix} \cos(\theta-\theta_r) & \sin(\theta-\theta_r) \\ -\sin(\theta-\theta_r) & \cos(\theta-\theta_r) \end{pmatrix} \begin{pmatrix} v_{\alpha r} \\ v_{\beta r} \end{pmatrix} \quad (24)$$

The ABC to DQ conversion implemented in SIMULINK is shown in Fig. 9.

STATOR AND ROTOR FLUX COMPUTATION

The standard stator and rotor equations for an induction machine, expressed in an arbitrary reference frame rotating at a speed ω_k are (Anderson, 1983)

$$\vec{v}_s\; R_s\, \vec{i}_r + \frac{d\vec{\lambda}_s}{dt} + j\omega_k\, \vec{\lambda}_s \text{ (stator equation)} \quad (25)$$

$$\vec{v}_r \; R_r \vec{i}_r + \frac{d\vec{\lambda}_r}{dt} + j(\omega_k - \omega_r)\vec{\lambda}_r \text{ (rotor equation)} \quad (26)$$

Where,

$\vec{v}_s \, \vec{v}_r$ = Stator and rotor voltage space vectors.

$\vec{\lambda}_s \, \vec{\lambda}_r$ = Stator and voltage flux linkage space vectors.

$\vec{i}_s \, \vec{i}_r$ = Stator and rotor current space vectors.

and ω_r = rotor angular speed.

The stator and rotor flux linkages can be expressed in terms of the stator and rotor currents and the self and mutual inductances as

$$\vec{\lambda}_s = L_s \vec{i}_s + L_m \vec{i}_r \quad (27)$$

$$\vec{\lambda}_r = L_m \vec{i}_s + L_r \vec{i}_r \quad (28)$$

Where,

L_s = Stator inductance.

L_r = Rotor inductance.

L_m = Mutual inductance.

Solving Eq. 27 and 28 for the stator and rotor currents and substituting in Eq. 25 and 26, we get

$$\frac{d\vec{\lambda}_r}{dt} = \vec{v}_s - \frac{R_s}{K}(L_s \vec{\lambda}_r - L_m \vec{\lambda}_r) - j\omega_k \vec{\lambda}_r \quad (29)$$

and

$$\frac{d\vec{\lambda}_r}{dt} = \vec{v}_r - \frac{R_r}{K}(L_s \vec{\lambda}_r - L_m \vec{\lambda}_s) - j(\omega_k - \omega_r)\vec{\lambda}_r \quad (30)$$

Where, $K = L_s L_r - Lm^2$.

Splitting Eq. 29 and 30 into their d and q components and rewriting in state space form,

$$\frac{d}{dt}\begin{bmatrix}\lambda_{ds}\\ \lambda_{qs}\\ \lambda_{dr}\\ \lambda_{qr}\end{bmatrix} = \begin{bmatrix} -\frac{R_s L_r}{k} & \omega_k & -\frac{R_s L_m}{k} & 0 \\ -\omega_k & -\frac{R_s L_r}{k} & 0 & -\frac{R_s L_m}{k} \\ -\frac{R_r L_m}{k} & 0 & -\frac{R_r L_s}{k} & (\omega_k - \omega_t) \\ 0 & -\frac{R_r L_m}{k} & (\omega_k - \omega_t) & -\frac{R_r L_s}{k} \end{bmatrix} \begin{bmatrix}\lambda_{ds}\\ \lambda_{qs}\\ \lambda_{dr}\\ \lambda_{qr}\end{bmatrix} \begin{bmatrix}v_{ds}\\ v_{qs}\\ v_{dr}\\ v_{qr}\end{bmatrix} \quad (31)$$

The above equation cannot be implemented directly in SIMULINK as a state space formulation, since the matrix is varying with time (due to the terms involving ω_r). The flux linkages obtained as the solution to the state space problem can be used to compute the currents using Eq. 27 and 28.

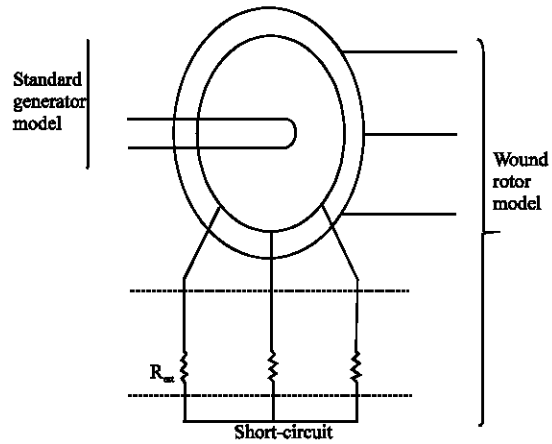

Fig. 10: Wound rotor induction machine model used for rotor resistance control

Electromagnetic torque computation: The electromagnetic Torque (T_e) produced by the induction machine can be expressed as

$$T_e = \frac{3}{2}\frac{P}{2}\frac{L_m}{L_s}\left(\vec{\lambda}_s \, \vec{i}_r^{\,*}\right) \quad (32)$$

Where, p = number of poles of the machine.

Squirrel cage induction machine model: In the squirrel cage induction machine, the rotor is short-circuited. Thus, by setting the rotor voltages to zero, the squirrel cage machine model is obtained.

Wound rotor induction machine model for rotor resistance control: In case of wound rotor machine model, an additional input is required, which corresponds to the external resistance added to the rotor circuit (Datta, 2002). Since the external resistance added is going to be the same in all the phases, the required model can be obtained by using (R_{ext} + R_r) in place of Rr in the equations and setting the rotor voltages to zero. The principle is illustrated in Fig. 10.

Doubly fed induction machine model: The doubly fed induction machine has current controlled rotor excitation. Thus, the rotor voltage equation is unnecessary, as the inputs are the stator voltage and rotor currents (Pena *et al*., 1996).

The stator current can be expressed as

$$\vec{i}_r = \frac{\vec{\lambda}_s - L_m \vec{i}_r}{L_s} \quad (33)$$

Using Eq. 27 and substituting Eq. 33 into 25 gives

$$\frac{d\vec{\lambda}_s}{dt} = \vec{v}_s - \frac{R_s}{L_s}\left(\vec{\lambda}_s - L_m \vec{i}_r\right) - j\omega k \vec{\lambda}_s \quad (34)$$

The above equation can be expressed in state space form as

$$\frac{d}{dt}\begin{bmatrix}\lambda_{ds}\\ \lambda_{qs}\end{bmatrix} = \begin{bmatrix}-\frac{R_s}{L_s} & \omega_k \\ -\omega_k & -\frac{R_s}{L_s}\end{bmatrix}\begin{bmatrix}\lambda_{ds}\\ \lambda_{qs}\end{bmatrix} + \begin{bmatrix}V_{ds} & \frac{R_s L_m}{L_s} i_{dr} \\ V_{qs} & \frac{R_s L_m}{L_s} i_{qr}\end{bmatrix} \quad (35)$$

Thus, by computing the stator flux linkage space vector, all the other currents and flux linkages can be computed.

RESULTS

The doubly fed induction generator is found to have least output power variation at high velocities, the output power variation is 20% and at low wind velocities, the output power variation is 10% and the fastest response of the three control techniques is simulated.

Moreover, the additional complexity of the system enables overall system power factor control, to help operate the system, at close to unity power factor. We can achieve almost unity power factors further research work is being carried out for deriving analytically wind power output in terms of RPM of rotor shaft. This will enable us to determine the rotor RPM at which wind power output is highest.

CONCLUSION

The mathematical modeling of the various components of the wind system (which are to be used to compare the control techniques) and their SIMULINK implementation have been investigated. The double feed introduction generator is vectorically found to be the best power control method with low losses, good performance and unity power factor operation.

REFERENCES

Datta, R. and V.T. Ranganathan, 2002. Variable speed wind power using doubly fed wound rotor induction machine-A comparison with aiternative scheme. IEEE. Trans Energy Conversion,17: 414-421.

Pena, R., J.C. Clare and G.M. Asher, 1996. A Doubly fed induction generator using back to back PWM converters supplying an Isolated Load from a variable speed wind turbines. IEEE. Pros. B. Electric Power Applications, 143: 380-387.

Sergey, A., Leonov Norwood, 2005. Mathematical Handbook for Electrical Engineers, Artech House Inc., 685 Conton street, MA 02062.

Siegfried Heir, Kassel University, Germany, 2006. Grid Integration of wind Energy conversion system, Second Edition John Wiley and Sons Ltd.

Simulink Manual, 1997.

Tony Burton, Powys, David Shape, Nick Jenkins and Ervin Bossany, 2001. Wind Energy hand book, John Wiley and Sons Ltd. Wai-kai Chen, 2005, The Electrical Engineering hand book, ELSEVEIR Acadamic Press.